Acute Respiratory Distress Syndrome Secondary to Inhalation of Chlorine Gas in Sheep

Andriy I. Batchinsky, MD, David K. Martini, MS, Bryan S. Jordan, MS, RN, Edward J. Dick, DVM, James Fudge, DVM, Candace A. Baird, RVT, Denise E. Hardin, AT, and Leopoldo C. Cancio, MD

Background: **Toxic industrial chemicals (TICs) are potential terrorist weapons. Several TICs, such as chlorine, act primarily on the respiratory tract, but knowledge of the pathophysiology and treatment of these injuries is inadequate. This study aims to characterize the acute respiratory distress syndrome (ARDS) caused by chlorine gas (Cl_2) inhalation in a large-animal model.**

Methods: **Anesthetized female sheep were ventilated with 300 L of a Cl_2/air/oxygen mixture for 30 minutes. In phase 1 (n = 35), doses were 0 ppm (Group 1, n = 6); 120 ppm (Group 2, n = 6); 240 to 350 ppm (Group 3, n = 11); and 400 to 500 ppm (Group 4, n = 12). In phase 2 (n = 17), doses were 0 ppm (Group 5, n = 5); 60 ppm (Group 6, n = 5); and 90 ppm (Group 7, n = 7), and the multiple inert gas elimination technique (MIGET) was used to characterize the etiology of hypoxemia. Computed tomography (CT) scans were performed daily for all animals.**

Results: **In Phase 1, lung function was well maintained in Group 1; Cl_2 caused immediate and sustained acute lung injury (Pao_2-to-FiO_2 ratio, PFR<3.0) in Group 2 and ARDS (PFR<2.0) in Groups 3 and 4. All animals in Groups 1 and 2 survived 96 hours. Kaplan-Meier analysis showed dose-related differences in survival (log-rank test, $p < 0.0001$). Logistic regression identified 280 ppm as the lethal dose 50%. CT and histopathology demonstrated lesions of both small airways and alveoli. In Phase 2, MIGET showed diversion of blood flow from normal to true-shunt lung compartments and, transiently, to poorly ventilated compartments.**

Conclusions: **Cl_2 causes severe, dose-related lung injury, with features seen in both smoke inhalation and in ARDS secondary to systemic disease. This model will be used to test new therapeutic modalities.**

Key Words: **Chlorine, Inhalation injury, Acute respiratory distress syndrome, Sheep, Multiple inert gas elimination technique, Computed tomography.**

J Trauma. 2006;60:944–957.

Recent world events raise concerns that toxic industrial chemicals (TICs) may be utilized as weapons of opportunity by terrorists. One of the most common TICs is chlorine. Chlorine is readily available; is transported daily in large quantities via water, road and rail; and was used as a weapon during previous wars. In addition, chlorine gas (Cl_2) spills from commercial cargo could rapidly expose large numbers of people, leading to severe acute lung injury (ALI) and adult respiratory distress syndrome (ARDS).[1]

Human research on Cl_2 exposure includes reports on war-related casualties,[2–4] observations of industrial[5–8] and other accidents,[9–14] and studies on the effects of Cl_2 on the lung[15] and other organs.[16–19] Animal research has been done on rhesus monkeys,[20] rabbits,[21] and rodents,[22–24] and recently on pigs.[25,26] These studies recognized Cl_2 as a potent irritant that causes toxic pulmonary edema and death,[27] and that in lower doses leads to reactive airway dysfunction syndrome (RADS).[28] To date, systemic[10,26,29] and inhaled steroids,[26,30,31] nebulized sodium bicarbonate,[32–34] humidified oxygen (O_2),[35] and beta agonists alone[35,36] and in combination with steroids[31] have all been suggested as treatment for Cl_2-associated pulmonary failure.

Current inhalation injury research is based on models employing smoke as the causative agent.[37–43] These studies have resulted in improvements in therapy such as high-frequency percussive ventilation leading to reductions in mortality.[40,44–46] The available inhalation injury models, however, are limited in severity by the development of carbon monoxide poisoning,[47] take 24 to 48 hours for the injury to unfold,[38,43,46,47] and, because of the complexity of smoke, may make interlaboratory comparisons difficult.[37]

The focus of this study was to develop a large-animal model of Cl_2 inhalation injury leading to ARDS that could be used for the development of new treatment modalities. Another objective of this study was to elucidate the mechanism of hypoxia following Cl_2 inhalation, both physiologically (by means of the multiple inert gas elimination technique [MIGET]) and morphologically (by means of computed tomography [CT] scanning). Our model addresses the limitations of the smoke inhalation models because no carbon monoxide is involved, the onset of injury takes only hours,

Submitted for publication November 1, 2005.
Accepted for publication January 6, 2006.
Copyright © 2006 by Lippincott Williams & Wilkins, Inc.
From the US Army Institute of Surgical Research, Fort Sam Houston, Texas.

The opinions or assertions contained herein are the private views of the authors and are not to be construed as official or as reflecting the views of the Department of the Army or the Department of Defense.

Funded by the Peer-Reviewed Medical Research Program, US Army Medical Research and Materiel Command, Ft. Detrick, Maryland (DAMD 17–03-2–0016).

Presented at the 64th Annual Meeting of the American Association for the Surgery of Trauma, September 22–24, 2005, Atlanta, Georgia.

Address for reprints: Library Branch, US Army Institute of Surgical Research, 3400 Rawley E. Chambers Avenue, Fort Sam Houston, TX 78234-6315; email: lee.cancio@amedd.army.mil.

DOI: 10.1097/01.ta.0000205862.57701.48

Copyright © Lippincott Williams & Wilkins. Unauthorized reproduction of this article is prohibited.

Report Documentation Page

Form Approved
OMB No. 0704-0188

Public reporting burden for the collection of information is estimated to average 1 hour per response, including the time for reviewing instructions, searching existing data sources, gathering and maintaining the data needed, and completing and reviewing the collection of information. Send comments regarding this burden estimate or any other aspect of this collection of information, including suggestions for reducing this burden, to Washington Headquarters Services, Directorate for Information Operations and Reports, 1215 Jefferson Davis Highway, Suite 1204, Arlington VA 22202-4302. Respondents should be aware that notwithstanding any other provision of law, no person shall be subject to a penalty for failing to comply with a collection of information if it does not display a currently valid OMB control number.

1. REPORT DATE	2. REPORT TYPE	3. DATES COVERED
01 MAY 2006	**N/A**	**-**

4. TITLE AND SUBTITLE	5a. CONTRACT NUMBER
Acute respiratory distress syndrome secondary to inhalation of chlorine gas in sheep	5b. GRANT NUMBER
	5c. PROGRAM ELEMENT NUMBER
6. AUTHOR(S)	5d. PROJECT NUMBER
Batchinsky, A. I. Martini, D. K. Jordan, B. S. Dick, E. J. Fudge, J. Baird, C. A. Hardin, D. E. Cancio, L. C.	5e. TASK NUMBER
	5f. WORK UNIT NUMBER
7. PERFORMING ORGANIZATION NAME(S) AND ADDRESS(ES)	8. PERFORMING ORGANIZATION REPORT NUMBER
United States Army Institute of Surgical Research, JBSA Fort Sam Houston, TX 78234	
9. SPONSORING/MONITORING AGENCY NAME(S) AND ADDRESS(ES)	10. SPONSOR/MONITOR'S ACRONYM(S)
	11. SPONSOR/MONITOR'S REPORT NUMBER(S)

12. DISTRIBUTION/AVAILABILITY STATEMENT
Approved for public release, distribution unlimited

13. SUPPLEMENTARY NOTES

14. ABSTRACT

15. SUBJECT TERMS

16. SECURITY CLASSIFICATION OF:			17. LIMITATION OF ABSTRACT	18. NUMBER OF PAGES	19a. NAME OF RESPONSIBLE PERSON
a. REPORT	b. ABSTRACT	c. THIS PAGE			
unclassified	**unclassified**	**unclassified**	**SAR**	**14**	

Table 1 Phase 1: Experimental Protocol

Time (hours)	Time Point	Event/Measurements/Techniques
–2.0	Surgical preparation	TIVA/surgical line placement
00.00	Baseline	Physiologic data recording. Vital sign collection, ABG, CT
0.5	Inhalation injury	0, 120, 240, 350, 400, 500 ppm Cl_2 (diluted in 100% O_2) injury in the negative pressure suite. Return to ICU
2.0	2 hours postinjury	Physiologic data recording. Vital sign collection, ABG, CT
Q6	Every 6 hours postinjury	Vital sign collection, ABG
Q24	Every 24 hours postinjury	Physiologic data recording. Vital sign collection, ABG, CT
96.0	96 hours postinjury	Physiologic data recording. Vital sign collection, ABG, CT. Termination of experiment, necropsy

and use of only one toxic component may simplify comparisons among laboratories.

MATERIALS AND METHODS

This study was approved by the US Army Institute of Surgical Research Animal Care and Use Committee and was carried out in accordance with the guidelines set forth by the Animal Welfare Act and other federal statutes and regulations relating to animals and studies involving animals and by the 1996 Guide for the Care and Use of Laboratory Animals of the National Research Council.

Experimental Design

This study was carried out in two phases. Phase 1 experiments lasted up to 96 hours, involved doses of 0 to 500 ppm of Cl_2 in 100% O_2, and had the primary goal of establishing the dose-related nature of the injury. (Dilution of Cl_2 with 100% O_2 was employed to ensure survival when high doses were used). The number of animals and doses used in this phase were: Group 1, n = 6, 0 ppm; Group 2, n = 6, 120 ppm; Group 3, n = 11, 240 to 350 ppm; and Group 4, n = 12, 400 to 500 ppm. Phase 2 experiments lasted 24 hours, involved doses of 0 to 90 ppm in 21% O_2, and had the primary goal of determining the etiology of hypoxia. The number of animals used and group-specific doses were: Group 5, n = 5, 0 ppm; Group 6, n = 5, 60 ppm; and Group 7, n = 7, 90 ppm. In phase 2, ventilation with room air was required to enable measurements of diffusion limitation (DL) by MIGET.[48] Lower doses were used to ensure survival of the animals when ventilated with 21% O_2. Unless otherwise specified, all approaches described below were identical for both phases of the experiment. Outlines of protocols and procedures for both phases are shown in Tables 1 and 2.

Animal Preparation

Fifty-two certified, nonpregnant female sheep weighing 43.3 ± 0.71 kg (phase 1, n = 35, 42.5 ± 0.9 kg; phase 2, n = 17, 44.91 ±1.1 kg) were quarantined for 1 week. On the day of study, the animals were anesthetized with isoflurane and underwent placement of a urinary catheter, tracheostomy, and lines in the right external jugular vein (REJV), right carotid artery, and left and right femoral arteries and veins. Enrofloxacin (Bayer, Shawnee Mission, KS), 100 g/mL, 1 mL BID IM, was given as prophylaxis on the day of surgery and every 24 hours. At completion of surgery, isoflurane was tapered off and total intravenous anesthesia (TIVA) was initiated (ketamine, 300 to 500 mcg/kg/min; midazolam, 1 mcg/kg/min) and continued throughout the experiment. Anesthesia levels were adjusted based on pinch tests and clinical assessment. When indicated, additional buprenorphine (Buprenex) 0.3 mg/kg IM was given for pain. The animals were transported to the intensive care unit (ICU) and mechanically ventilated (see Ventilator Management below).

Table 2 Phase 2: Experimental Protocol

Time (hours)	Time Point	Event/Measurements/Techniques
–2.0	Surgical preparation	TIVA/surgical line placement
00.00	Baseline	FiO_2 21%, MIGET, physiologic data recording. Vital sign collection, ABG, CT
0.5	Inhalation injury	0, 60, 90 ppm Cl_2 (diluted in 21% O_2) injury in the negative pressure suite. Return to ICU
0.5	30 minutes postinjury	FiO_2 21%, MIGET, physiologic data recording. Vital sign collection, ABG
1.0	1 hour postinjury	FiO_2 21%, MIGET, physiologic data recording. Vital sign collection, ABG
2.0	2 hours postinjury	FiO_2 21%, MIGET, physiologic data recording. Vital sign collection, ABG,CT
Q6	Every 6 hours postinjury	Vital sign collection, ABG
24	24 hours postinjury	FiO_2 21%, MIGET, physiologic data recording. Vital sign collection, ABG,CT, termination of experiment, necropsy

TIVA, induction of total intravenous anesthesia; FiO_2, fraction of inspired oxygen; %ABE, arterial blood gasses; CT, computed tomography; MIGET, multiple inert gas elimination technique.

Copyright © Lippincott Williams & Wilkins. Unauthorized reproduction of this article is prohibited.

Physiologic Measurements

Cardiac output (CO), systemic vascular resistance, and stroke volume were indexed to body surface area according to Meeh's formula: body surface area (m^2) = 0.09*(weight, kg)$^{0.667}$. Arterial blood gases (ABG) were measured with an i-STAT blood gas analyser (Abbot Laboratories, East Windsor, NJ). A pulmonary arterial (PA) catheter (7 F, Model 41239–04-05, Abbott, Chicago, IL) was inserted via the REJV. Bolus thermodilution CO and pulmonary artery wedge pressure (PAWP) were determined at each time point. Electrocardiogram (ECG), pulse oximetry (SpO_2) (Datex Ohmeda True Tech Plus 3900), central venous pressure (CVP), peripheral arterial pressure (PAP), and arterial blood pressure (ABP) waveforms were continuously displayed using a clinical monitor (Viridia CMS 2000, Boeblingen, Germany). Pressures were transduced (Transpac IV, Abbott, Chicago, IL) at heart level. Physiologic data were digitally recorded at specified time points (Tables 1 and 2).[49]

Cl_2 Injury

Inhalation injury occurred in a dedicated suite under negative-pressure conditions. The procedure was developed in cooperation with the Brooke Army Medical Center safety office. Ambient sampling was used (detector head GM-PS-6A-H; sensor GM-CDS-6-CL10-R; Matheson Tri Gas, Chicago, IL) to detect gas leaks (none occurred). Personnel performing Cl_2 delivery wore full-face fitted gas masks. A custom gas mix consisting of Cl_2 1000 ppm, balance medical air, was obtained (#G2659698, Matheson Tri Gas). Using a mass flow blender (MMIX-0116-XX, Matheson Tri Gas) the gas was diluted to the desired concentration with 100% medical O_2 for phase 1 and medical air for phase 2. Cl_2 was delivered via tracheostomy with an Ambu bag at a tidal volume (TV) of 1000 mL, respiratory rate (RR) of 10/min for 30 minutes, yielding 300 L. Expired air was passed through a Boeringer scavenger to a charcoal canister (Precision Filtration Products, Pennsburg, PA), and was evacuated via the institutional vacuum system. After exposure to Cl_2, the animals were transported back into the ICU.

ICU Management Postinjury

The ventrally recumbent position was employed for all animals. TIVA with deep sedation was carried out during the study, rendering most of the subjects unconscious throughout the duration of the protocol. Maintenance intravenous (IV) fluids (lactated Ringers solution, 0.9% sodium chloride, 5% dextrose) were given throughout the study: 4 mL/kg for the first 10 kg of body weight, 2 mL/kg for the next 10 kg, and 1 mL/kg for each additional kg. Rate was adjusted to maintain a 0.5 to 1 mL/kg/hr urine output.

Ventilator Management

Phase 1

A Servo 300-A (Siemens-Elemia, Sweden) mechanical ventilator was used. Delivered gases were heated and humidified. Volume control mode was used with a standard of 5 cm H_2O positive end expiratory pressure (PEEP) and a goal for oxygenation of at least 90% by arterial blood hemoglobin O_2 saturation (SpO_2 and/or Sao_2). Settings were as follows. The fraction of inspired O_2 concentration (FiO_2) $\geq$50%, and was adjusted to maintain SpO_2 $\geq$90% and partial pressure of O_2 in arterial blood (Pao_2) $>$60 mm Hg. The target for peak inspiratory pressure (PIP) was $\leq$40 cm H_2O. The target for pH was $\geq$7.25. Baseline TV settings were 13 mL/kg. If arterial pH was greater than 7.25, TV was lowered by 2 to 3 mL/kg steps to keep PIP below 40 cm H_2O. If pH was below 7.25, decreases in TV were avoided, and a higher PIP was accepted. Baseline RR was 15/min. TV and RR were adjusted to maintain the arterial level of CO_2 (P_aCO_2) between 30 and 45 mm Hg. To prevent atelectasis, when in hypocapnia and low to normal PIP, the RR was dialed down before TV adjustments were made. If PIP was high, TV was decreased first to keep PIP below 40 cm H_2O followed by RR adjustments. Achievement of these goals required hourly ventilator adjustments during the first 6 hours postinjury. In groups 1 and 2, semihourly to hourly suctioning had to be carried out in the first 6 hours postinjury with, on average, 2 to 4 mL of tracheal fluid retrieved at each occasion. The need for suctioning and ventilator adjustments became less frequent after the first 24 hours postinjury and was less intense in more severely injured in groups 3 and 4, possibly reflecting extensive necrosis.

Phase 2

A humidified circuit was not used to avoid condensation of expired inert gases and influence on MIGET results. FiO_2 was kept at 21% for injury and at all times when MIGET sampling took place. At all other times, the approach was identical to the one described for phase 1.

Multiple Inert Gas Elimination Technique

The MIGET was carried out according to the method of Wagner et al.[50] Details of our MIGET technique have been described elsewhere.[51] Briefly, a 1-L bag of 5% dextrose was saturated by six inert gases: SF_6, ethane, cyclopropane, halothane, ethyl ether, and acetone. This infusate was administered IV at a constant rate of half the minute ventilation rate expressed in mL/min. During sampling time points, 7 mL of arterial blood and 30 mL of mixed expired air were collected into airtight glass syringes. Gas chromatography (GC) was used to determine the levels of the inert gases in the expired air and arterial blood. The obtained GC, ABG, oxygen consumption (VO_2), carbon dioxide production (VCO_2), CO, minute ventilation (Ve), body temperature, room temperature, and individual inert gas solubility data (determined experimentally for each of the gases) were entered into custom software provided by Dr. Wagner. Mixed venous levels of the six gases were calculated by the software. The retention (ratio of the arterial to mixed venous levels) and excretion (ratio of the expired to mixed venous levels) of each gas

Copyright © Lippincott Williams & Wilkins. Unauthorized reproduction of this article is prohibited.

were represented as a function of solubility in blood. Ventilation-perfusion (V/Q) ratio was assessed graphically and numerically.

CT Scan Acquisition and Analysis

Chest CT scans were performed at full inspiration during baseline as well as 2, 24, 48, 72 and 96 hours postinjury in phase 1 (Table 1) and at baseline, 2, and 24 hours postinjury in phase 2 (Table 2). A spiral CT scanner (Aquillion TSX-101A, Toshiba, Irvine, CA) was used and 0.5-mm thick images acquired at 120 Kv and 350 mA. Semiautomated image analysis was performed using the software package, 3D-Doctor (Able Software Corp., Lexington, MA) as previously reported by our group.[52,53] The pulmonary parenchyma was separated into four regions based on the Hounsfield unit (HU) ranges reported by Gattinoni et al.[54] Hyperinflated (–1000 to –900 HU), normally aerated (–900 to –500 HU), poorly aerated (–500 to –100 HU), and nonaerated areas (–99 to +100 HU) were defined by the software in each of the slices for each of the lungs. In Phase 1 animals, grayscale-density histograms were constructed and the severity of injury assessed at baseline, 2 hours, and 24 hours postinjury using a single CT scan slice obtained 1 to 2 cm above the diaphragm, which has been reported to be representative of overall injury severity in ARDS.[55] The single slice, obtained and analyzed in our study, resided in close vicinity to the area where histologic samples were taken from the right middle lobe.

Experiment Termination, Necropsy, and Specimen Collection

Animals were euthanized 96 hours after injury in phase 1 and 24 hours after injury in phase 2 (or sooner in the event of imminent death [MAP <30 mm Hg for 30 minutes]) by an overdose of sodium pentobarbital (Fatal-Plus, Dearborn, MI). Dorsal sections of the middle lobe in the right lung were harvested, fixed in formalin, and processed for hematoxylin and eosin staining and light microscopical examination. For five animals in phase 2, the volumes of pleural effusions were measured and the respective protein contents determined.

Statistics

SPSS version 10.1 (Chicago, IL) and Microsoft Excel (Redmond, WA) were used for analysis. For phase 1, survival was assessed at 96 hours. Survival data were subjected to stepwise logistic regression analysis (backwards likelihood ratio method) to generate a model predictive of survival under conditions of this study. Kaplan-Meier analysis was performed to examine the effect of dose on survival time. Physiologic data from phases 1 and 2 were analyzed by repeated measures analysis of variance (ANOVA), General Linear Model. For phase 1, post-hoc Dunnett's *t* tests were used to compare each injured group to the control group at each time point. For phase 2, the smaller number of control animals (five) mandated that post-hoc paired-samples *t* tests be used to compare each group's values at 1 and 24 hours after injury to baseline conditions; *p* values were Bonferroni-corrected for two nonorthogonal comparisons. Data are presented as means ± SEM. Significance was accepted at $p < 0.05$.

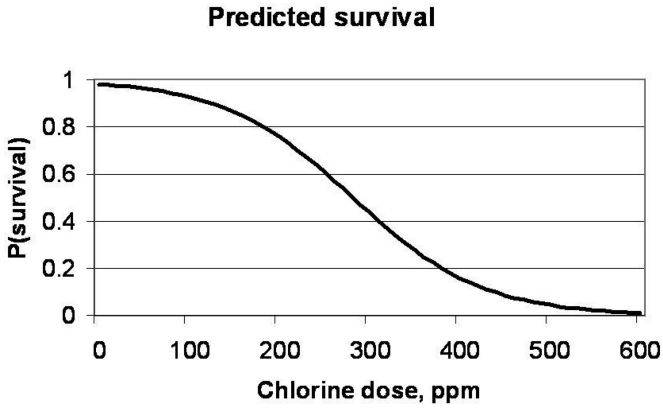

Fig. 1. *Phase 1: The calculated LD50 based on this model was 280 ppm, as can be estimated by visual inspection of this graph.*

RESULTS

Phase 1

A total of 1,761 hours of ICU time were used to complete the phase 1 of this study. All animals in Groups 1 and 2 lived through 96 hours. Logistic regression analysis produced the following equation predictive of survival to 96 hours:

$$p\,(\text{survival}) = e^k/(1+e^k), \text{ where } k = -0.014 \times \text{dose} + 3.939$$

Based on this equation, the lethal dose 50% (LD 50) was determined to be 280 ppm (Fig. 1). Kaplan-Meier analysis was used to examine the effect of dose on survival time. For this analysis, 0-ppm and 120-ppm animals (Groups 1 and 2), none whom died before 96 hours, were considered together and a significant effect of dose on survival time was found leading to a survival of 5 of 11 subjects in group 3 (240 to 350 ppm) and only 2 of 12 subjects in group 4 (400 to 500 ppm) (Fig. 2).

Pao_2-to-FiO_2 ratio (PFR) was well preserved in the mechanically ventilated control group throughout the 96-hour study. Dose-related decreases in PFR were evident immediately after injury (Fig. 3). In Group 2, these values reached ALI levels (PFR <3.0) at the 2-hour point and on average remained in this range throughout the study. Group 3 and 4 values reached ARDS levels (PFR<2.0) at the 2-hour point and in general remained at this level in survivors for 96 hours. In all injured groups, the time course for this variable was biphasic: there was a nadir at 2 hours, followed by a partial recovery by about 10 to 24 hours, followed by a decline. Changes in blood pressure followed a similar time course. Mean arterial pressure (MAP) was fairly constant in control animals (Table 3). Injury produced a dose-related drop in MAP. MAP in less severely injured animals in Group 2 recovered more quickly (by 18 hours) than in surviving ani-

Copyright © Lippincott Williams & Wilkins. Unauthorized reproduction of this article is prohibited.

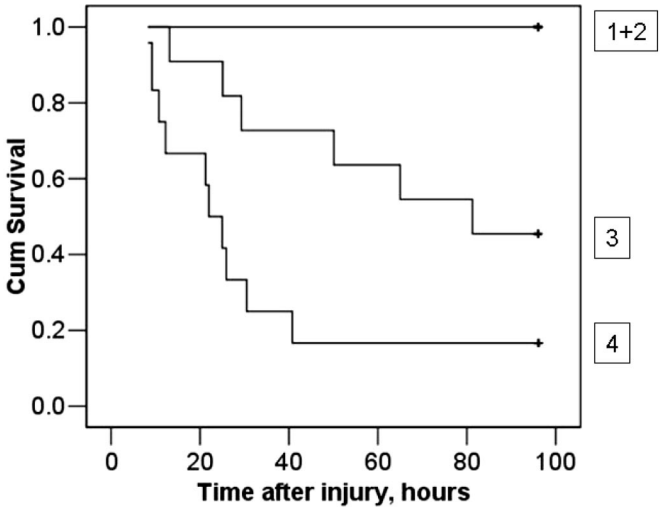

Fig. 2. *Phase 1: Kaplan-Meier survival curves. Groups 1 and 2, 0 to 120 ppm; group 3, 240 to 350 ppm; group 4, 400 to 500 ppm. Log-rank test,* $p < 0.0001$ *for overall comparison; Group 1 and 2 versus Group 3,* $p = 0.0032$*; Group 1 and 2 versus Group 4,* $p < 0.0001$*; Group 3 versus Group 4,* $p = 0.0291$.

mals in Groups 3 and 4, where it returned to control levels by 48 hours. A similar phenomenon was observed for the cardiac index (Table 3) and the stroke volume index (data not shown). Tachycardia was not seen; in fact, there was a statistically nonsignificant decrease in heart rate with injury. The systemic vascular resistance index (SVRI) appeared to increase slightly with injury, although this change was not significant (Table 3). PIP increased during the course of the study when compared to controls in animals in Groups 3 and 4 (Table 3). By the end of the study, the PIP in group 3 returned to control levels, whereas in group 4 PIP levels remained significantly elevated (Table 3). Changes in $PaCO_2$, PAP, and PAWP were not significant (data not shown).

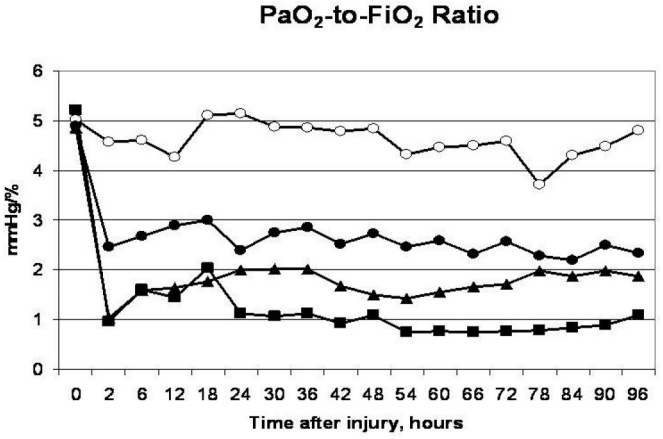

Fig. 3. *Phase 1: Pao_2-to FiO_2 ratio (PFR) as a function of time after injury for four dose groups. ○ Group 1, 0 ppm; ● Group 2, 120 ppm; ▲ Group 3, 240 to 350 ppm; ■ Group 4, 400 to 500 ppm. See also Table 3 for statistical significance of these differences.*

CT scan analysis data obtained from the baseline, 2-hour, and 24-hour postinjury time points in phase 1 are shown in Table 4. This table gives the fraction of the total number of pixels consistent with hyperaerated, normally aerated, poorly aerated, or nonaerated tissue in each lung slice examined. Exposure to Cl_2 decreased the fraction of normal lung tissue by 2 hours, which persisted at 24 hours. The decrease in normal lung tissue was particularly marked in Group 4. Concomitantly, there was an increase in poorly and nonaerated lung tissue.

As illustrated in Figure 4, exposure to Cl_2 led to the development of characteristic "window-frost" or "feathery" density distributions along the bronchial tree. At 2 hours postinjury, animals developed ARDS, featuring ground glass opacification and patchy consolidation. Cl_2 inhalation resulted in the development of a characteristic ARDS feature: a marked downsizing of the volume of normal lung that has been termed "baby lung."[56] With time, further progression of the disease could be traced as the densities broadened, became confluent and culminated in widely spread consolidated areas. Bilateral pleural effusions were evident (Fig. 4, C to F).

In controls, as well as at baseline time points for all animals, density-based analysis of single-slice CT scans revealed the pulmonary parenchyma to be almost fully allocated within the normally aerated compartments (HU: –900 to –500). With progression of time in the uninjured animals, this unimodal pattern remained the same (Fig. 5A). In those injured, a rightward shift along the histogram was evident and a bimodal graphical appearance emerged, representing an increase in poorly- and nonaerated areas within the lung (Fig. 5B).

Phase 2

A total of 408 hours of ICU time were required to complete phase 2. All phase 2 animals survived. CT and physiologic data in phase 2 followed the same trends as in phase 1; however, changes were less marked, reflecting lesser injury (data not shown). PaO_2 was nearly halved at 30 minutes and continued to drop reaching a nadir at 2 hours (Table 5). As in phase 1, there was an improvement in Pao_2 around 12 to 24 hours, returning to levels not significantly different from baseline by 24 hours in the 60-ppm group (Table 5). The most striking finding from the MIGET analysis was an early increase in blood flow to the true shunt compartment in both injury groups, which was sustained through 24 hours (Table 5, Fig. 6). There was also an increase in blood flow to the very low (V/Q 0 to 0.01) and low (V/Q 0.01 to 0.1) compartments, which, by contrast with true shunt, resolved by 24 hours (Table 5, Fig. 6). This redistribution of blood flow to shunt, very low, and low V/Q compartments occurred at the expense of blood flow to the normal V/Q compartment (V/Q 0.1 to 1). Meanwhile, blood flow to the high (V/Q 1 to 10) and very high (V/Q 10 to 100) compartments increased in group 6 but did not change in group 7 (Table 5). Marked dispersion and skewness of V/Q distributions were present

Copyright © Lippincott Williams & Wilkins. Unauthorized reproduction of this article is prohibited.

Table 3 Phase 1: Hemodynamic and Pulmonary Data

Variable	Group	Baseline	2 Hours	6 Hours	12 Hours	18 Hours	24 Hours	36 Hours	48 Hours	72 Hours	96 Hours
PFR	1	5.02 ± 0.22	4.57 ± 0.48	4.61 ± 0.32	4.27 ± 0.67	5.11 ± 0.25	5.15 ± 0.28	4.86 ± 0.24	4.83 ± 0.42	4.59 ± 0.46	4.81 ± 0.33
	2	4.89 ± 0.18	2.46 ± 0.69*	2.68 ± 0.66*	2.90 ± 0.60	3.00 ± 0.65†	2.39 ± 0.73*	2.85 ± 0.63*	2.74 ± 0.64*	2.57 ± 0.69†	2.33 ± 0.72*
	3	4.86 ± 0.28	1.03 ± 0.25‡	1.60 ± 0.25‡	1.63 ± 0.32‡	1.77 ± 0.32‡	2.00 ± 0.43‡	2.02 ± 0.34‡	1.51 ± 0.19‡	1.72 ± 0.27*	1.87 ± 0.20*
	4	5.12 ± 0.21	0.95 ± 0.11‡	1.58 ± 0.17‡	1.46 ± 0.13‡	1.95 ± 0.46‡	1.08 ± 0.25‡	1.12 ± 0.28‡	1.09 ± 0.07*	0.77 ± 0.25*	1.09 ± 0.60*
PIP	1	20 ± 2	20 ± 1	21 ± 2	21 ± 3	17 ± 2	21 ± 3	21 ± 2	20 ± 2	20 ± 1	21 ± 2
	2	16 ± 1	20 ± 1*	19 ± 2	19 ± 1	18 ± 1	19 ± 1	20 ± 1	21 ± 2	18 ± 1	19 ± 1
	3	19 ± 1	27 ± 2	25 ± 1	25 ± 2	27 ± 3*	27 ± 2	24 ± 3	26 ± 3	27 ± 4	18 ± 5
	4	16 ± 1	23 ± 2	24 ± 1	27 ± 1	30 ± 2†	37 ± 3†	31 ± 5	31 ± 1†	40 ± 6†	40 ± 6†
MAP	1	126 ± 8	119 ± 3	121 ± 8	112 ± 7	117 ± 6	123 ± 8	116 ± 5	119 ± 9	114 ± 12	113 ± 12
	2	139 ± 6	79 ± 8‡	74 ± 4‡	67 ± 4‡	91 ± 11‡	95 ± 8	104 ± 9	93 ± 6	107 ± 8	84 ± 12
	3	126 ± 4	62 ± 5‡	69 ± 7‡	65 ± 6‡	75 ± 5‡	70 ± 8‡	86 ± 7†	86 ± 8	87 ± 10	80 ± 13
	4	127 ± 4	46 ± 3‡	54 ± 3‡	49 ± 4‡	53 ± 5‡	49 ± 10‡	77 ± 2†	89 ± 45	66 ± 24	75 ± 39
CI	1	3.2 ± 0.3	3.5 ± 0.2	3.4 ± 0.3	3.3 ± 0.3	3.2 ± 0.3	3.1 ± 0.3	3.8 ± 0.4	3.7 ± 0.4	3.6 ± 0.4	3.3 ± 0.4
	2	4.7 ± 0.4†	2.3 ± 0.2†	2.2 ± 0.7‡	2.2 ± 0.2†	3.4 ± 0.5	3.6 ± 0.4	4.2 ± 0.6	4.2 ± 0.3	4.6 ± 0.3	4.4 ± 0.3
	3	3.6 ± 0.2	1.7 ± 0.2‡	1.7 ± 0.1‡	1.8 ± 0.1‡	2.2 ± 0.2	2.7 ± 0.4	3.2 ± 0.1	4.3 ± 0.4	4.6 ± 0.5	4.1 ± 0.5
	4	3.1 ± 0.3	1.4 ± 0.3‡	1.2 ± 0.1‡	1.2 ± 0.2‡	1.7 ± 0.2*	1.9 ± 0.3	3.0 ± 0.3	2.8 ± 0.8	3.5 ± 0.0	3.9 ± 0.7
SVRI	1	3156 ± 369	2778 ± 170	2853 ± 223	2802 ± 338	3001 ± 236	3263 ± 301	2520 ± 244	2564 ± 342	2581 ± 405	2818 ± 551
	2	2440 ± 177	2771 ± 200	2775 ± 347	2435 ± 305	2212 ± 327	2093 ± 187*	1995 ± 161	1724 ± 118	1830 ± 126	1454 ± 212†
	3	2983 ± 237	3211 ± 299	3255 ± 255	2861 ± 265	2704 ± 229	2128 ± 172*	2111 ± 145	1678 ± 253	1528 ± 140†	1542 ± 247
	4	3501 ± 224	3768 ± 686	3684 ± 283	3316 ± 217	2551 ± 277	1968 ± 281*	1947 ± 540	2243 ± 690	1339 ± 599	1308 ± 657

p values from Dunnett's *t* test, comparing groups 2, 3, and 4 to group 1 at each time point.
*$p < 0.01$.
†$p < 0.05$.
‡$p < 0.001$.

Copyright © Lippincott Williams & Wilkins. Unauthorized reproduction of this article is prohibited.

Table 4 Phase 1: Computed Tomography Scan Data

Variable	Group	Baseline	2 Hours	24 Hours
Hyper	1	0.12 ± .04	0.19 ± 0.03	0.17 ± 0.03
	2	0.01 ± 0.01	0.04 ± 0.01*	0.01 ± 0.01*
	3	0.15 ± 0.03	0.09 ± 0.01†	0.07 ± 0.02†
	4	0.19 ± 0.01	0.11 ± 0.01‡	0.04 ± 0.01*
Normal	1	0.78 ± 0.02	0.73 ± 0.01	0.76 ± 0.02
	2	0.78 ± 0.08	0.42 ± 0.03*	0.37 ± 0.04†
	3	0.69 ± 0.03	0.48 ± 0.06†	0.45 ± 0.08†
	4	0.73 ± 0.01	0.42 ± 0.02*	0.25 ± 0.05*
Poor	1	0.07 ± 0.01	0.06 ± 0.02	0.05 ± 0.01
	2	0.15 ± 0.07	0.21 ± 0.04†	0.17 ± 0.02
	3	0.12 ± 0.03	0.20 ± 0.03†	0.15 ± 0.02‡
	4	0.05 ± 0.01	0.27 ± 0.02*	0.24 ± 0.03*
Non	1	0.03 ± 0.01	0.02 ± 0.01	0.02 ± 0.01
	2	0.06 ± 0.01	0.33 ± 0.02*	0.45 ± 0.04†
	3	0.04 ± 0.01	0.23 ± 0.05†	0.33 ± 0.08†
	4	0.03 ± 0.00	0.20 ± 0.02†	0.49 ± 0.06*

Group 1 is sham injury, group 2 is 120 ppm, group 3 is 240 to 350 ppm, group 4 is 400 to 500 ppm. *p* values from Dunnet's *t* test, comparing groups 2, 3, and 4 to group 1.

Hyper, fraction of pixels in the lung slice with Hounsfield Unit (HU) values in the hyperaerated range; normal, fraction of pixels in the normally aerated range; poor, fraction of pixels in the poorly aerated range; non, fraction of pixels in the nonaerated range.

*$p < 0.001$.

†$p < 0.01$.

‡$p < 0.05$.

after Cl_2 inhalation as evidenced by increased log SDQ above 0.6 (normal level)[57] and in many cases above 2.0, attesting to injury severity (Table 5). Figure 6 depicts examples of V/Q changes over time in an injured subject. Increases in dead space ventilation and diffusion limitation were not features of this injury. The excellent correlation ($r^2=0.9959$) between the measured arterial pO_2 and the arterial pO_2 predicted by the MIGET proves that full alveolar arterial equilibration took place at times of sampling (Fig. 7), thus excluding diffusion limitation as a cause of hypoxia in this model.

Pathology Results

Histopathologically, both small airway and alveolar-capillary membrane lesions were observed. The histologic features in animals exposed to 60 to 120 ppm (Fig. 8, A and B for an example of changes in an animal exposed to 120 ppm) were localized regional necrosis of bronchiolar epithelium with variable congestion of capillaries, edema, fibrin deposition, and acute inflammation. In phase 1, in survivors, macrophages became more prevalent in the inflammatory response and some bronchiolar epithelial regeneration was present; however, alveolar edema persisted. Lesions became more penetrating and widespread with increasing injury severity (Fig. 8). When exposed to higher doses of Cl_2 (Fig. 8, C and D; nonsurvivor shown), necrosis, edema, fibrin deposition, and inflammation all extended into the adjacent alveoli, and lesions developed that involved entire lung sections. The amount of edema and necrosis increased as a function of injury severity and time. Pleural effusions were a consistent finding in all groups (mean protein content 3 ± 0.21 g/dL) as measured in five of the phase 2 animals. The mean volume of these exudates was 121.6 ± 19.39 mL and 41.7 ± 10.7 mL in the right and left hemithoraxes, respectively, further substantiating our empirical observation that a systematic preponderance of the injury to the right lung took place.

DISCUSSION

In sheep, exposure to Cl_2 resulted in: 1) pathophysiologically, the development of true shunt and V/Q mismatch; 2) clinically, a dose-dependent decrease in PFR, transient hypotension and decreased cardiac output; and 3) morphologically, a typical "feathery" appearance on CT with progressive development to confluent consolidation in the lung, reflecting extensive alveolar flooding and necrosis. In this model, Cl_2 inhalation injury led to a rapid and dose-dependent development of ARDS with an estimated lethal dose 50% of 280 ppm at 96 hours. In humans, levels of 46 to 60 ppm have resulted in toxic pneumonitis and pulmonary edema, 430 ppm was lethal after 30 minutes, and 1,000 ppm caused death within a few minutes.[1] In their porcine large-animal model of Cl_2 injury, Gunnarsson et al. reported a 50% mortality at 6 hours after exposure to 140 ppm using 20-kg pigs.[25] Our LD50 was higher, possibly reflecting differences in patient management and/or in interspecies tolerance to the injury.

Cl_2 exposure involves a variety of moieties such as elemental Cl_2, hydrochloric acid, hypochlorous acid, and chloramines.[27] Cl_2 is rapidly hydrolized into hypochlorous acid, which may act as one of the mediators of Cl_2 toxicity[58] damaging cellular integrity,[2] reacting with sulfhydryl groups in proteins,[23,59,60] and inhibiting enzymes.[23,59,61] Disruption of cell-wall integrity and increased permeability[59] can also

Copyright © Lippincott Williams & Wilkins. Unauthorized reproduction of this article is prohibited.

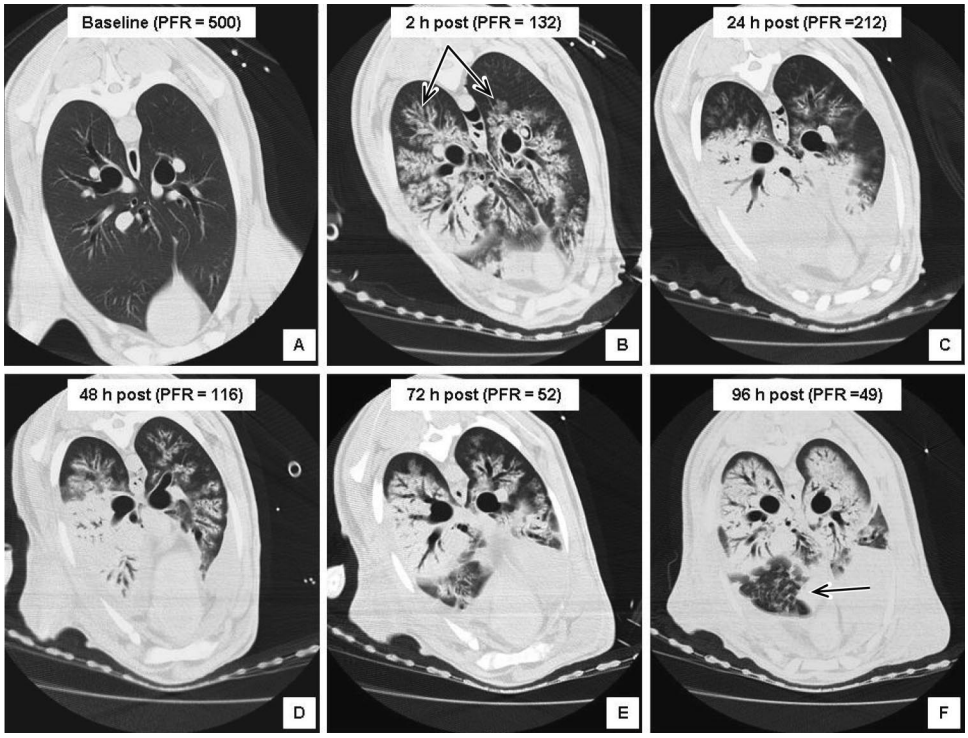

Fig. 4. *Lung computed tomography. Progression of injury over time in an injured animal (#109, 400 ppm, survivor). (A) Baseline, PFR=500, normal lung. (B) 2-hour postinjury, PFR=132, Cl_2-induced ARDS. Note the "window frost" or "feathery" appearance of increased density areas along the bronchial tree; (arrows) diffuse parenchymal inhomogeneity; marked decrease in the volume of normally aerated lung. (C) 24-hour postinjury, PFR = 212. Confluent gravity-dependent consolidation and ground glass opacification with predominance to the right lung; bilateral pleural effusion. (D) 48-hour postinjury, PFR=116. "Feathery" and confluent consolidation, pleural exudates. (E) 48-hour postinjury, PFR=52. Same features as in (D). Note the gravity-independent distribution of consolidated areas. Improved local lung aeration on the right side. (F) 96-hour postinjury, PFR=49. Identical features as in (E). Further improvement in aeration (arrow). End of study.*

cause edema and direct local tissue destruction[3,5] and clinically may yield to hypoxia.

Hypoxia is the hallmark of Cl_2 inhalation injury.[27] The specific cause of hypoxia is underinvestigated. Shimazu et al., using MIGET, found that V/Q mismatch, more than an increase in true shunt, accounted for the hypoxia secondary to smoke inhalation.[62] In their pig model, Gunnarson et al. suggested that significant V/Q mismatching may account for the decrease in oxygenation seen in Cl_2 injury.[25] Increased true shunt with little or no blood flow increase to the low V/Q areas were implicated in alloxan and oleic acid canine models of ARDS[63,64] as well as in a porcine model of unilateral pulmonary contusion by Proctor et al.[65] and an adaptation of that model by our laboratory (unpublished data). Our MIGET findings suggest that hypoxia secondary to Cl_2 is caused by a more penetrating and multifactorial injury than smoke inha-

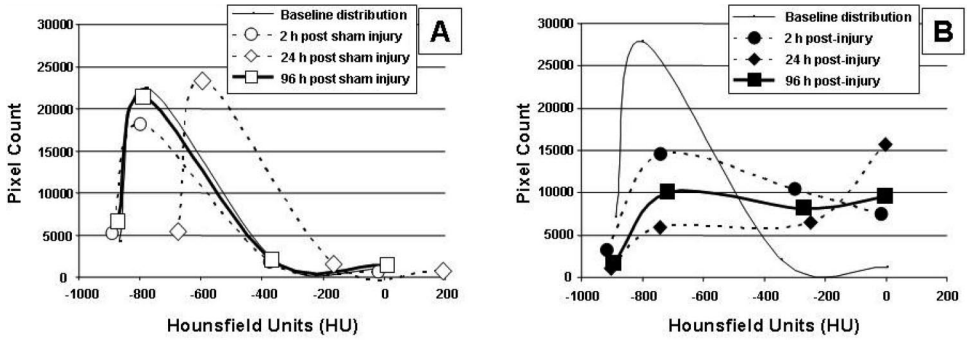

Fig. 5. *Phase 1: One-slice CT histogram analysis of right lung slices from 1 to 2 cm above the diaphragm. (A) Control animals. Most of the lung tissue is well aerated as evidenced by the unimodal distribution of aeration zones within the –900 to –500 compartment. Minimal amount of poorly (HU window of –500 to –100) and nonaerated (HU window of –100 to 100) lung. (B) Injured animals, Group 4. Note a rightward shift in the density distribution representing developed poorly and nonaerated compartments in the lung.*

Copyright © Lippincott Williams & Wilkins. Unauthorized reproduction of this article is prohibited.

Table 5 Phase 2: MIGET DATA

Variable	Group	Baseline	30 Minutes	1 Hour	2 Hours	24 Hours
PaO_2	5	97.3 ± 4.0	100.1 ± 6.7	99.9 ± 8.2	102.0 ± 4.9	87.1 ± 2.0
	6	92.1 ± 2.3	55.0 ± 5.6	49.8 ± 6.2*	47.3 ± 3.3	70.2 ± 15.0
	7	92.3 ± 6.7	48.6 ± 5.2	40.9 ± 2.7†	44.4 ± 3.7	59.0 ± 6.2‡
$Q_{\text{true shunt}}$	5	1.02 ± 0.27	1.58 ± 0.55	2.13 ± 0.86	2.08 ± 0.90	2.38 ± 0.88
	6	2.02 ± 0.67	14.18 ± 4.37	33.22 ± 4.39*	45.22 ± 4.93	39.84 ± 6.07*
	7	3.31 ± 0.73	23.13 ± 8.78	37.17 ± 7.07*	45.24 ± 6.48	44.50 ± 6.66*
$Q_{\text{V/Q 0 to 0.01}}$	5	0.00 ± 0	0.00 ± 0	0.00 ± 0	0.00 ± 0	0.00 ± 0
	6	0.00 ± 0	10.72 ± 1.94	8.28 ± 2.22‡	1.26 ± 0.83	0.32 ± 0.32
	7	0.00 ± 0	9.93 ± 1.18	9.83 ± 1.22†	4.66 ± 0.95	0.79 ± 0.48
$Q_{\text{V/Q 0.01 to 0.1}}$	5	0.00 ± 0	0.00 ± 0	0.00 ± 0	0.00 ± 0	0.00 ± 0
	6	4.22 ± 2.01	13.64 ± 3.93	8.82 ± 2.76	0.94 ± 0.65	1.50 ± 1.03
	7	1.47 ± 0.85	16.16 ± 1.14	12.96 ± 2.68‡	5.76 ± 1.74	1.61 ± 0.96
$Q_{\text{V/Q 0.1 to 1}}$	5	90.12 ± 3.14	92.75 ± 4.21	93.13 ± 4.20	92.62 ± 2.26	84.68 ± 7.09
	6	87.60 ± 3.29	49.78 ± 9.50	39.50 ± 8.51‡	39.98 ± 7.92	35.06 ± 8.07‡
	7	88.44 ± 2.44	35.99 ± 9.27	25.14 ± 4.97†	21.89 ± 3.55	36.34 ± 7.39†
$Q_{\text{V/Q 1 to10}}$	5	8.64 ± 3.32	5.48 ± 4.50	4.53 ± 4.43	5.10 ± 2.55	12.86 ± 6.80
	6	6.12 ± 1.97	11.00 ± 2.52	9.48 ± 2.15‡	11.62 ± 2.57	22.74 ± 5.37‡
	7	14.89 ± 8.73	13.97 ± 3.52	14.43 ± 2.31	21.07 ± 4.02	16.40 ± 1.71
$Q_{\text{V/Q 10 to 100}}$	5	0.16 ± 0.08	0.18 ± 0.18	0.20 ± 0.07	0.16 ± 0.07	0.10 ± 0.10
	6	0.00 ± 0	0.66 ± 0.20	0.76 ± 0.08†	0.96 ± 0.23	0.52 ± 0.29
	7	0.36 ± 0.15	0.84 ± 0.15	0.47 ± 0.17	1.41 ± 0.37	0.30 ± 0.17
Mean Q	5	0.62 ± 0.01	0.58 ± 0.06	0.58 ± 0.06	0.61 ± 0.05	0.57 ± 0.10
	6	0.39 ± 0.03	0.24 ± 0.07	0.26 ± 0.07	0.61 ± 0.05	0.87 ± 0.15‡
	7	0.49 ± 0.05	0.19 ± 0.03	0.21 ± 0.03*	0.55 ± 0.13	0.68 ± 0.06
$logSD_Q$	5	0.45 ± 0.04	0.40 ± 0.05	0.42 ± 0.02	0.39 ± 0.04	0.51 ± 0.04
	6	0.70 ± 0.10	1.84 ± 0.17	1.81 ± 0.27‡	1.13 ± 0.25	0.89 ± 0.23
	7	0.61 ± 0.06	2.93 ± 0.83	2.21 ± 0.07†	1.96 ± 0.15	1.08 ± 0.18‡
Skewness Q	5	0.20 ± 0.07	0.18 ± 0.12	0.25 ± 0.08	0.18 ± 0.08	0.05 ± 0.07
	6	−0.09 ± 0.07	−2.64 ± 1.67	−2.70 ± 1.44	−2.14 ± 1.93	−1.27 ± 1.50
	7	0.15 ± 0.17	−1.22 ± 1.86	−3.54 ± 1.13‡	−5.62 ± 0.90	−1.74 ± 0.97

Group 5 is sham injury, group 6 is 60 ppm, group 7 is 90 ppm. *p* values are for post-hoc paired-samples *t* tests, comparing data at hour 1 and hour 24 to hour 0.

‡$p < 0.05$.

*$p < 0.01$.

†$p < 0.001$.

PaO_2, partial pressure of oxygen in arterial blood, mm Hg; $Q_{\text{true shunt}}$, percentage of the cardiac output (Q) pertaining to the true shunt compartment, V/Q=0; $Q_{\text{V/Q 0 to 0.01}}$, Q to the compartment for which the V/Q ratio is between 0 and 0.01, etc; Mean V/Q, mean value of V/Q on a logarithmic scale for the function, Q = f(V/Q) (see text); $logSD_Q$, second moment (logarithmic standard deviation) of this function; skewness Q, third moment of this function.

lation as it causes both small airway injury (manifested by V/Q mismatch) *and* alveolar injury (manifested by development of true shunt). MIGET data presented here are reminiscent of human studies of ARDS in which the injury is seen as multifactorial, involving shunting, alveolar flooding and V/Q mismatch[66] with distribution of blood flow to low V/Q areas.[66,67] Low V/Q areas in ARDS may represent alveoli that are poorly ventilated (edematous and/or partially flooded) but still perfused.[66,67] This pool of unstable alveoli could become either completely atelectatic (adding to the amount of true shunt) or, if recruited, subsequently provide for areas of normal V/Q matching.[66] The latter may have accounted for the transient relative improvement in oxygenation occurring between 2 hours and 24 hours in phase 2. This can be inferred from the MIGET results that revealed the blood flow to low and very low V/Q areas seen during the 2 hours postinjury to be absent at 24 hours. We propose that before the final decline in oxygenation took place, the potentially recruitable alveoli became fully engaged in oxygenation, leading to improvements in PFR. Recruitment of these "unstable" alveoli with PEEP may have therapeutic implications.[68]

Reports on roentgenographic findings in Cl_2-induced ALI have not been consistent, generally suggesting lower airway injury[3] and citing vascular congestion, patchy consolidation and pulmonary edema as morphologic features.[27] To our knowledge, ours is the first study utilizing quantitative evaluation of density distributions following Cl_2 inhalation injury. The "window-frost" or "feathery" density pattern reported here is a visual manifestation of the peribronchial edema indicative of small airway injury. These radiologic patterns may be an early and distinctive feature of corrosive penetrating alveolar injuries caused by hydrophilic agents such as Cl_2. With time, these initial features develop into widely distributed ground-glass opacification and pulmonary consolidation. The total consolidation in ARDS has been

Copyright © Lippincott Williams & Wilkins. Unauthorized reproduction of this article is prohibited.

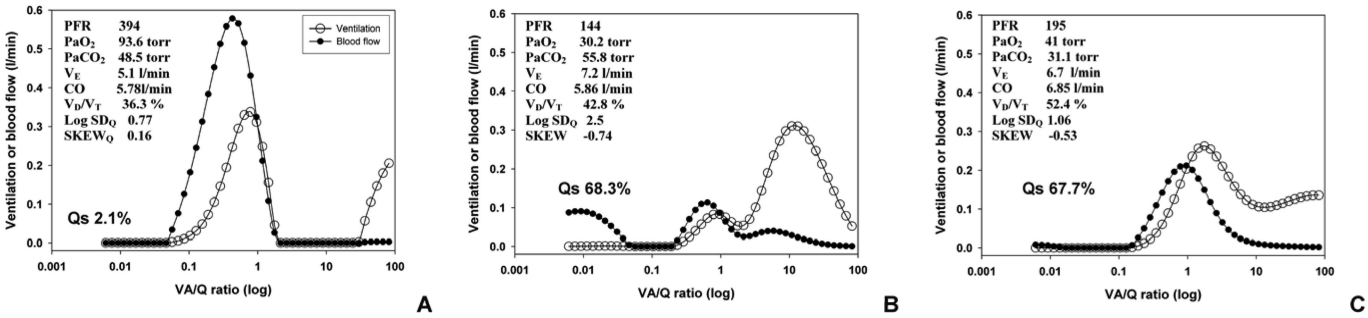

Fig. 6. *Distributions of ventilation (V) and perfusion (Q) as a function of V/Q ratio in an animal exposed to 90 ppm of Cl_2. (A) Baseline. V/Q ratio is normal and centered around 1. V and Q distributions are well matched and the amount of true shunt is low and within normal physiologic limits. (B) 2 hours postinjury. Note severe V/Q mismatch, blood flow to very low and low V/Q areas and a true shunt of 68% of CO, marked dispersion (scatter) and skewness of the V and Q distributions. (C) 24-hours postinjury. Shunt remained unchanged however the V/Q matching improved as the blood flow to low and very low V/Q areas became redistributed to normally aerated segments of the lung.*

found to be correlated with Pao_2 and shunt fraction.[55] Our histographic analysis showed predominantly bimodal density distributions as a reflection of developing ground glass opacification (likely representing edema and atelectasis) and some gravity-dependent and independent consolidation (signs of alveolar injury and flooding), all attesting to the severe pulmonary inhomogeneity post-Cl_2 injury. Indeed, Gattinoni et al. and Maunder et al. found that the lung in ARDS is inhomogeneous.[69,70] When one considers the patchy mosaic of the alternating unaffected areas versus the unventilated/consolidated areas typically seen in ARDS, one should expect most of the TV to be delivered to the ventilated lung areas, thus accentuating volu- and barotrauma and, arguably, resulting in hyperinflation of these open lung units.[71,72] The lung units available for ventilation in ARDS have been called "baby lung," referring to their small volume compared with normal lung volume. Importantly, this diminished lung has been described as small rather than stiff.[56] The TV redistribution into a small volume postinjury appears to be crucial in the accentuation of the ventilator-induced insult in ARDS and has been suggested to be a causative factor in the development of emphysema-like air-space enlargement, pseudocysts, and bronchiectasis as manifestations of barotrauma in patients with severe ARDS.[73]

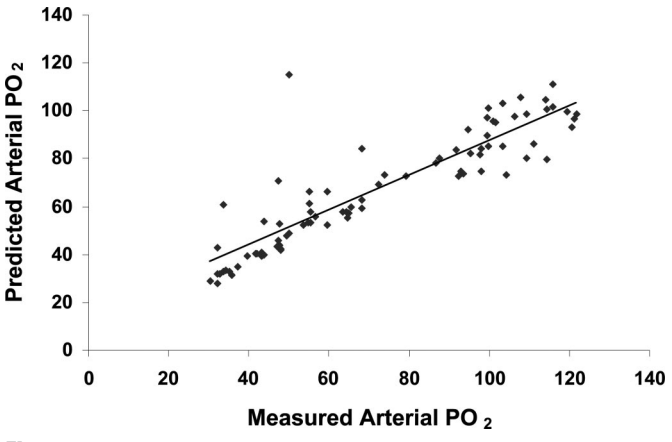

Fig. 7. *Measured Pao_2 plotted against the Pao_2 predicted by MIGET $r^2 = 0.7956$, $n = 164$. (see text).*

Histopathologically, Cl_2-induced pulmonary injury was less severe and more localized in phase 2, most likely as a reflectance of exposure to lower doses of Cl_2. Findings included: edema, vascular congestion, and acute inflammation with some bronchiolar epithelial regeneration. When exposed to increasing doses of Cl_2, the necrosis, edema, fibrin deposition and inflammation extended into the adjacent alveoli with the most severe lesions involving entire lung sections. Others have reported on similar, but nonspecific findings.[74] Canine studies published by Winternitz in 1920[75] showed histopathologic progression through several stages, from lung edema and acute alveolar inflammation through pulmonary congestion and hemorrhage and into extensive bronchiolar mucosal destruction, atelectasis, pneumonia, and obliterative bronchiolitis. Gunnarsson et al. stated that the exposure of distal airways to Cl_2 could have caused increased capillary leakage and extravasation of fluids as mechanisms of the injury.[30] The latter may lead to the development of pleural effusions,[76–78] attesting to inadequacy of natural pathways for the resolution of pulmonary edema.[79]

As is true for any model, ours had its limitations. General anesthesia has been reported to influence gas exchange, pulmonary circulation, and airway secretion clearance mechanisms.[80] It is unknown if TIVA used in our study caused similar effects. Mechanical ventilation most likely had an effect in our study and prevented the animals' natural defense mechanisms—such as apnea, shallow breathing, coughing, and sneezing—from acting in face of exposure to a potent irritant such as Cl_2. Bypassing of the upper respiratory tract via tracheostomy probably led to the lung being exposed to a higher gas concentration, because Cl_2 could not have been cleared from the inhaled air by the respiratory mucosa.[58] Ventilator-associated lung injury may have been a significant factor in this injury model as evidenced by the visual presence of the hyperinflated areas and air trapping in the CT scans. Finally, although the purposeful standardiza-

Copyright © Lippincott Williams & Wilkins. Unauthorized reproduction of this article is prohibited.

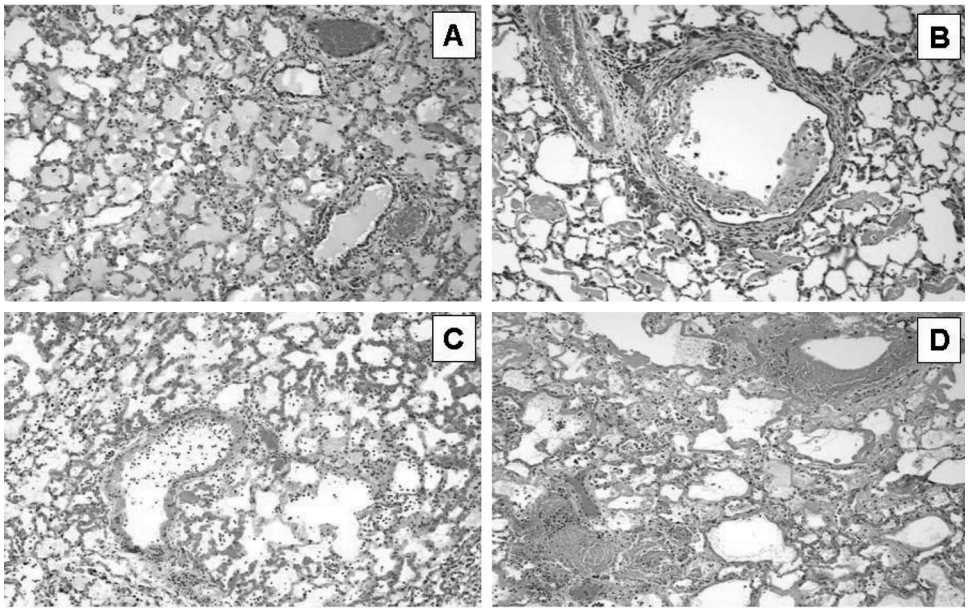

Fig. 8. *Histologic progression of Cl_2-induced lung injury (H&E). (A) 120-ppm dose. Note extensive airway edema, mild acute inflammation, necrosis of bronchiolar epithelium and diffuse capillary congestion. (B) 120-ppm dose. Note organizing fibrino-cellular debris in bronchiolar and alveolar lumens. There is necrosis and loss of the bronchiolar epithelium with incomplete squamous regeneration. Thickening of the alveolar septa present and mild inflammatory response are present. (C) Severe injury, nonsurvivor, 500 ppm, 21 hours after injury. Diffuse complete necrosis of bronchioles and alveolar septa. Prominent diffuse capillary congestion, acute inflammation and edema. (D) Severe injury, nonsurvivor, 240 ppm, 40 hours postinjury. Diffuse complete necrosis of all structures present. Marked thickening of alveolar septa and filling of the alveolar and bronchial lumen with necrotic debris and inflammatory cells.*

tion to a single injurious agent in this inhalation injury model has, in comparison to smoke models, led to advantages in the reproducibility of the injury, it could also be argued that the work is mostly applicable to severe cases of Cl_2 inhalation injury in unconscious spontaneously breathing subjects.

CONCLUSIONS

The findings presented in this manuscript may further our understanding of Cl_2 injury in particular and of ARDS secondary to exposure to toxic hydrophilic gases. Cl_2 causes an injury with features seen in both smoke inhalation (small airway lesions manifested by V/Q mismatch) and in ARDS secondary to systemic disease and pulmonary contusion (alveolar-endothelial lesions featuring an increase in true shunt). The results of this study also support the current view that the lung in ARDS may be severely inhomogeneous, thus reiterating the importance of judicious use of supplemental O_2, PEEP and, most importantly, application of small tidal volume ventilation as an approach to decreasing mortality and as a means for lung rest. Further studies will be directed at understanding the biochemistry of chlorine injury and at exploring new treatment modalities.

REFERENCES

1. Balmes JR. Acute pulmonary injury from hazardous materials. In: Sullivan J, Krieger G, eds. Hazardous Materials Toxicology: Clinical Principles of Environmental Health; 2000.
2. Stockholm International Peace Research Institute. The problem of chemical and biological warfare. A study of the historical, technical, military, legal, and political aspects of CBW and possible disarmament measures. In: The Rise of CB Weapons. New York: Humanities Press; 1971.
3. Freitag L, Firusian N, Stamatis G, Greschuchna D. The role of bronchoscopy in pulmonary complications due to mustard gas inhalation. *Chest.* 1991;100:1436–1441.
4. Haber LF. The poisonous cloud. Chemical warfare in the First World War. Oxford: Clarendon Press; 1986.
5. Lemiere C, Malo JL, Boutet M. Reactive airways dysfunction syndrome due to chlorine: sequential bronchial biopsies and functional assessment. *Eur Respir J.* 1997;10:241–244.
6. Leroyer C, Malo JL, Infante-Rivard C, Dufour JG, Gautrin D. Changes in airway function and bronchial responsiveness after acute occupational exposure to chlorine leading to treatment in a first aid unit. *Occup Environ Med.* 1998;55:356–359.
7. Salisbury DA, Enarson DA, Chan-Yeung M, Kennedy SM. First-aid reports of acute chlorine gassing among pulpmill workers as predictors of lung health consequences. *Am J Ind Med.* 1991;20:71–81.
8. Winder C. The toxicology of chlorine. *Environ Res.* 2001;85:105–114.
9. Baxter PJ, Davies PC, Murray V. Medical planning for toxic releases into the community: the example of chlorine gas. *Br J Ind Med.* 1989;46:277–285.
10. Fleta J, Calvo C, Zuniga J, Castellano M, Bueno M. Intoxication of 76 children by chlorine gas. *Hum Toxicol.* 1986;5:99–100.
11. Sexton JD, Pronchik DJ. Chlorine inhalation: the big picture. *J Toxicol Clin Toxicol.* 1998;36:87–93.
12. Wood BR, Colombo JL, Benson BE. Chlorine inhalation toxicity from vapors generated by swimming pool chlorinator tablets. *Pediatrics.* 1987;79:427–430.
13. Minami M, Katsumata M, Miyake K, et al. Dangerous mixture of

Copyright © Lippincott Williams & Wilkins. Unauthorized reproduction of this article is prohibited.

household detergents in an old-style toilet: a case report with simulation experiments of the working environment and warning of potential hazard relevant to the general environment. *Hum Exp Toxicol.* 1992;11:27–34.
14. Traub SJ, Hoffman RS, Nelson LS. Case report and literature review of chlorine gas toxicity. *Vet Hum Toxicol.* 2002;44:235–239.
15. Rotman HH, Fliegelman MJ, Moore T, et al. Effects of low concentrations of chlorine on pulmonary function in humans. *J Appl Physiol.* 1983;54:1120–1124.
16. Morris JB, Wilkie WS, Shusterman DJ. Acute respiratory responses of the mouse to chlorine. *Toxicol Sci.* 2005;83:380–387.
17. Schins RP, Emmen H, Hoogendijk L, Borm PJ. Nasal inflammatory and respiratory parameters in human volunteers during and after repeated exposure to chlorine. *Eur Respir J.* 2000;16:626–632.
18. Shusterman D, Balmes J, Murphy MA, Tai CF, Baraniuk J. Chlorine inhalation produces nasal airflow limitation in allergic rhinitic subjects without evidence of neuropeptide release. *Neuropeptides.* 2004;38:351–358.
19. Kilburn KH. Chlorine-induced damage documented by neurophysiological, neuropsychological, and pulmonary testing. *Arch Environ Health.* 2000;55:31–37.
20. Klonne DR, Ulrich CE, Riley MG, et al. One-year inhalation toxicity study of chlorine in rhesus monkeys (Macaca mulatta). *Fundam Appl Toxicol.* 1987;9:557–572.
21. Menaouar A, Anglade D, Baussand P, et al. Chlorine gas induced acute lung injury in isolated rabbit lung. *Eur Respir J.* 1997; 10:1100–1107.
22. Martin JG, Campbell HR, Iijima H, et al. Chlorine-induced injury to the airways in mice. *Am J Respir Crit Care Med.* 2003;168:568–574.
23. McNulty MJ, Chang JC, Barrow CS, Casanova-Schmitz M, Heck HD. Sulfhydryl oxidation in rat nasal mucosal tissues after chlorine inhalation. *Toxicol Lett.* 1983;17:241–246.
24. Wolf DC, Morgan KT, Gross EA, et al. Acute respiratory responses of the mouse to chlorine. *Toxicol Sci.* 2005;83:380–387.
25. Gunnarsson M, Walther SM, Seidal T, Bloom GD, Lennquist S. Exposure to chlorine gas: effects on pulmonary function and morphology in anaesthetised and mechanically ventilated pigs. *J Appl Toxicol.* 1998;18:249–255.
26. Wang J, Winskog C, Edston E, Walther SM. Inhaled and intravenous corticosteroids both attenuate chlorine gas-induced lung injury in pigs. *Acta Anaesthesiol Scand.* 2005;49:183–190.
27. Das R, Blanc PD. Chlorine gas exposure and the lung: a review. *Toxicol Ind Health.* 1993;9:439–455.
28. Donnelly SC, FitzGerald MX. Reactive airways dysfunction syndrome (RADS) due to chlorine gas exposure. *Ir J Med Sci.* 1990; 159:275–276.
29. Chester EH, Kaimal J, Payne CB, Jr, Kohn PM. Pulmonary injury following exposure to chlorine gas. Possible beneficial effects of steroid treatment. *Chest.* 1977;72:247–250.
30. Gunnarsson M, Walther SM, Seidal T, Lennquist S. Effects of inhalation of corticosteroids immediately after experimental chlorine gas lung injury. *J Trauma.* 2000;48:101–107.
31. Wang J, Zhang L, Walther SM. Administration of aerosolized terbutaline and budesonide reduces chlorine gas-induced acute lung injury. *J Trauma.* 2004;56:850–862.
32. Bosse GM. Nebulized sodium bicarbonate in the treatment of chlorine gas inhalation. *J Toxicol Clin Toxicol.* 1994;32:233–241.
33. Chisholm CD, Singleton EM, Okerberg CV. Inhaled sodium bicarbonate therapy for chlorine inhalation injuries. *Ann Emerg Med.* 1989;18:466.
34. Douidar SM. Nebulized sodium bicarbonate in acute chlorine inhalation. *Pediatr Emerg Care.* 1997;13:406–407.
35. Guloglu C, Kara IH, Erten PG. Acute accidental exposure to chlorine gas in the Southeast of Turkey: a study of 106 cases. *Environ Res.* 2002;88:89–93.
36. Wang J, Zhang L, Walther SM. Inhaled budesonide in experimental chlorine gas lung injury: influence of time interval between injury and treatment. *Intensive Care Med.* 2002;28:352–357.
37. Prien T, Traber DL. Toxic smoke compounds and inhalation injury–a review. *Burns Incl Therm Inj.* 1988;14:451–460.
38. Shimazu T, Yukioka T, Hubbard GB, et al. A dose-responsive model of smoke inhalation injury. Severity-related alteration in cardiopulmonary function. *Ann Surg.* 1987;206:89–98.
39. Walker HL, McLeod CG, Jr., McManus WF. Experimental inhalation injury in the goat. *J Trauma.* 1981;21:962–964.
40. Cioffi WG, deLemos RA, Coalson JJ, Gerstmann DA, Pruitt BA, Jr. Decreased pulmonary damage in primates with inhalation injury treated with high-frequency ventilation. *Ann Surg.* 1993;218:328–335.
41. Ogura H, Cioffi WG, Jr., Jordan BS, et al. The effect of inhaled nitric oxide on smoke inhalation injury in an ovine model. *J Trauma.* 1994;37:294–301; discussion 301–292.
42. Harrington DT, Jordan BS, Dubick MA, et al. Delayed partial liquid ventilation shows no efficacy in the treatment of smoke inhalation injury in swine. *J Appl Physiol.* 2001;90:2351–2360.
43. Alpard SK, Zwischenberger JB, Tao W, et al. New clinically relevant sheep model of severe respiratory failure secondary to combined smoke inhalation/cutaneous flame burn injury. *Crit Care Med.* 2000;28:1469–1476.
44. Sheridan RL, Zapol WM, Ritz RH, Tompkins RG. Low-dose inhaled nitric oxide in acutely burned children with profound respiratory failure. *Surgery.* 1999;126:856–862.
45. Cox CS, Jr., Zwischenberger JB, Traber DL, et al. Heparin improves oxygenation and minimizes barotrauma after severe smoke inhalation in an ovine model. *Surg Gynecol Obstet.* 1993;176:339–349.
46. Tasaki O, Dubick MA, Goodwin CW, Pruitt BA, Jr. Effects of burns on inhalation injury in sheep: a 5-day study. *J Trauma.* 2002; 52:351–357.
47. Tasaki O, Goodwin CW, Saitoh D, et al. Effects of burns on inhalation injury. *J Trauma.* 1997;43:603–607.
48. Torre-Bueno JR, Wagner PD, Saltzman HA, Gale GE, Moon RE. Diffusion limitation in normal humans during exercise at sea level and simulated altitude. *J Appl Physiol.* 1985;58:989–995.
49. Koenig SC, Woolard C, Drew G, et al. Integrated data acquisition system for medical device testing and physiology research in compliance with good laboratory practices. *Biomed Instrum Technol.* 2004;38:229–240.
50. Wagner PD, Saltzman HA, West JB. Measurement of continuous distribution of ventilation-perfusion ratios: theory. *J Appl Physiol.* 1974;36:588–599.
51. Batchinsky AI, Cancio LC. The multiple inert gas elimination technique: current methodology at the U.S. Army Institute of Surgical Research. USAISR Technical Report 2002. National Technical Information Service. Available at http://www.ntis.gov. Accessed February 10, 2006. ADA 411984.
52. Batchinsky AI, Cancio LC. Semiautomatic three-dimensional reconstruction and quantitative analysis of pulmonary CT scans: current methodology at the U.S. Army Institute of Surgical Research. Technical Report 2002. National Technical Information Service. Available at http://www.ntis.gov. Accessed February 10, 2006. ADA 412026.
53. Park MS, Cancio LC, Batchinsky AI, et al. Assessment of severity of ovine smoke inhalation injury by analysis of computed tomographic scans. *J Trauma.* 2003;55:417–427.
54. Gattinoni L, Caironi P, Pelosi P, Goodman LR. What has computed tomography taught us about the acute respiratory distress syndrome? *Am J Respir Crit Care Med.* 2001;164:1701–1711.
55. Goodman LR, Fumagalli R, Tagliabue P, et al. Adult respiratory distress syndrome due to pulmonary and extrapulmonary causes: CT,

Copyright © Lippincott Williams & Wilkins. Unauthorized reproduction of this article is prohibited.

clinical, and functional correlations. *Radiology.* 1999;213:545–552.
56. Gattinoni L, Pesenti A. The concept of "baby lung." *Intensive Care Med.* 2005;31:776–784.
57. Marshall BE, Hanson CW, Frasch F, Marshall C. Role of hypoxic pulmonary vasoconstriction in pulmonary gas exchange and blood flow distribution. 2. Pathophysiology. *Intensive Care Med.* 1994; 20:379–389.
58. Nodelman V, Ultman JS. Longitudinal distribution of chlorine absorption in human airways: comparison of nasal and oral quiet breathing. *J Appl Physiol.* 1999;86:1984–1993.
59. Chlorine and Hydrogen Chloride. In: Safety IPoC. Environmental Health Criteria 21. Geneva: World Health Organization; 1982.
60. Knox WE, Stumpf PK, Green DE, Auerbach VH. The inhibition of sulfhydryl enzymes as the basis of the bactericidal action of chlorine. *J Bacteriol.* 1948;55:451–458.
61. Pereira WE, Hoyano Y, Summons RE, Bacon VA, Duffield AM. Chlorination studies. II. The reaction of aqueous hypochlorous acid with alpha-amino acids and dipeptides. *Biochim Biophys Acta.* 1973; 313:170–180.
62. Shimazu T, Yukioka T, Ikeuchi H, et al. Ventilation-perfusion alterations after smoke inhalation injury in an ovine model. *J Appl Physiol.* 1996;81:2250–2259.
63. Schoene RB, Robertson HT, Thorning DR, et al. Pathophysiological patterns of resolution from acute oleic acid lung injury in the dog. *J Appl Physiol.* 1984;56:472–481.
64. Wagner PD, Laravuso RB, Goldzimmer E, Naumann PF, West JB. Distribution of ventilation-perfusion ratios in dogs with normal and abnormal lungs. *J Appl Physiol.* 1975;38:1099–1109.
65. Moomey CB, Jr., Fabian TC, Croce MA, Melton SM, Proctor KG. Cardiopulmonary function after pulmonary contusion and partial liquid ventilation. *J Trauma.* 1998;45:283–290.
66. Dantzker DR, Brook CJ, Dehart P, Lynch JP, Weg JG. Ventilation-perfusion distributions in the adult respiratory distress syndrome. *Am Rev Respir Dis.* 1979;120:1039–1052.
67. Markello R, Winter P, Olszowka A. Assessment of ventilation–perfusion inequalities by arterial–alveolar nitrogen differences in intensive-care patients. *Anesthesiology.* 1972;37:4–15.
68. Gattinoni L, Caironi P, Carlesso E. How to ventilate patients with acute lung injury and acute respiratory distress syndrome. *Curr Opin Crit Care.* 2005;11:69–76.
69. Gattinoni L, D'Andrea L, Pelosi P, et al. Regional effects and mechanism of positive end-expiratory pressure in early adult respiratory distress syndrome. *JAMA.* 1993;269:2122–2127.
70. Maunder RJ, Shuman WP, McHugh JW, Marglin SI, Butler J. Preservation of normal lung regions in the adult respiratory distress syndrome. Analysis by computed tomography. *JAMA.* 1986; 255:2463–2465.
71. Puybasset L, Cluzel P, Gusman P, et al. Regional distribution of gas and tissue in acute respiratory distress syndrome. I. Consequences for lung morphology. CT Scan ARDS Study Group. *Intensive Care Med.* 2000;26:857–869.
72. Rouby JJ, Puybasset L, Cluzel P, Richecoeur J, Lu Q, Grenier P. Regional distribution of gas and tissue in acute respiratory distress syndrome. II. Physiological correlations and definition of an ARDS Severity Score. CT Scan ARDS Study Group. *Intensive Care Med.* 2000;26:1046–1056.
73. Rouby JJ, Lherm T, Martin de Lassale E, et al. Histologic aspects of pulmonary barotrauma in critically ill patients with acute respiratory failure. *Intensive Care Med.* 1993;19:383–389.
74. Adelson L, Kaufman J. Fatal chlorine poisoning: report of two cases with clinicopathologic correlation. *Am J Clin Pathol.* 1971;56:430–442.
75. Winternitz MC, Lambert RA, Jackson L, Smith GH. The pathology of chlorine poisoning. In: Winternitz MC, ed. Collected Studies on the Pathology of War Gas Poisoning. New Haven: Yale University Press;1920:1–31.
76. Aberle DR, Wiener-Kronish JP, Webb WR, Matthay MA. Hydrostatic versus increased permeability pulmonary edema: diagnosis based on radiographic criteria in critically ill patients. *Radiology.* 1988;168:73–79.
77. Ware LB, Matthay MA. The acute respiratory distress syndrome. *N Engl J Med.* 2000;342:1334–1349.
78. Wiener-Kronish JP, Matthay MA. Pleural effusions associated with hydrostatic and increased permeability pulmonary edema. *Chest.* 1988;93:852–858.
79. Rosenberg AL. Fluid management in patients with acute respiratory distress syndrome. *Respir Care Clin N Am.* 2003;9:481–493.
80. Wagner PD, Dueck R. Mechanisms of abnormal gas exchange during anesthesia. *Int J Clin Monit Comput.* 1984;1:59–71.

DISCUSSION

Dr. Saman Arbabi (Ann Arbor, Michigan): Drs. Batchinsky, Cancio, and colleagues have characterized an animal model of ARDS in response to chlorine gas inhalation.

The severity of injury can be adjusted depending on chlorine gas concentration, and the model appears to be reproducible. The authors have done detailed studies to define the pathophysiological response to injury as it correlates to outcomes.

Their detailed description and study of V/Q mismatch and shunt in response to chlorine gas inhalation is outstanding. The statistical analyses are flawless.

However, similar to any model of injury, the main question that remains unanswered is the relevance to true clinical scenarios. One of the goals of this study was to characterize a clinically relevant model.

Did the authors mean a clinically relevant model for chlorine gas inhalation, or was their goal to look at inhalation injury in general or ARDS in general?

While this model may be applicable to chlorine gas inhalation, it appears to have significant differences from smoke inhalation. It has much more rapid onset.

Chlorine is one dimensional compared to the complex nature of smoke. Because of tracheostomy, which was used in these experiments, there was no upper airway injury.

I agree with the authors that the less complex chlorine gas model is more reliable and is reproducible and there is an excellent dose dependent profile.

But because of simplicity and uniformity, the more reliable models are often less clinically relevant. What evidence do the authors have that their model is relevant to a patient with smoke inhalation or ARDS?

Since some of the injury is due to hydrochloric acid, is there any similarity to aspiration injury models since HCl was used in these models? The third question is did you look at pulmonary cytokine production and neutrophil sequestration either in BAL or lung homogenates? Does this model induce SIRS?

The authors suggested that the transient improvement in oxygenation may be related to recruitment of atelectatic al-

Copyright © Lippincott Williams & Wilkins. Unauthorized reproduction of this article is prohibited.

veoli. Could they see this recruitment phenomenon in this CT scan?

Dr. Andriyl I. Batchinsky (San Antonio, Texas): The relevance of our model to true clinical scenarios is limited to the methods we used and the model as it was constructed. I would say that our focus was to answer some of the questions with regard to pathophysiology of chlorine injury and also to build a rapid-in-onset model of ARDS that could be potentially used as such for investigation of new treatment modalities. The findings presented here may be mostly relevant to ARDS secondary to toxic hydrophilic corrosive inhalants and, clinically, applicable to severe cases of chlorine inhalation injury in unconscious spontaneously breathing patients.

There are conclusions from this work that may be relevant with respect to ARDS in general, such as CT phenomena of recruitment of previously fully consolidated lung represented in the CT slide. We have also found that the blood flow to areas with very low V/Q ratios in this model resolved by 24 hours. Analogous results were reported by Dantzker et al. when they used MIGET in human ARDS patients. The mentioned phenomenon physiologically may represent a pool of potentially recruitable alveoli that could be engaged. These are the two main relevant factors to ARDS inferred from our results.

The relevance to patients with smoke inhalation injury is as follows. Both smoke and chlorine are injuring the lungs in the same site—in the small airways, with chlorine additionally damaging the alveolar-capillary membrane. Pathophysiologically, there is some overlap based on MIGET data between the two models. In their comprehensive investigation of smoke inhalation injury in sheep, Shimazu et al. have found V/Q mismatch to be the main factor in the hypoxia secondary to smoke inhalation. The group also identified moderate shunt, albeit not significant enough to explain the hypoxia in full. However, chlorine as a corrosive agent and very hydrophilic in nature may elicit a much more pronounced local tissue damage, potentially leading to complete necrosis and alveolar capillary membrane injury, thus constituting to an overall more penetrating and severe injury.

Are there any similarities with aspiration injury models induced by hydrogen chloride? Both of these agents may act locally eliciting corrosive tissue damage and leading to necrosis through dissolution in water and formation of acidic components. The work of Dantzker et al. that I referred to with respect to MIGET findings in humans addressed this question to a degree. There were 16 patients in that study, and 6 of them had ARDS secondary to aspiration. Pathophysiologically, the data looked similar to the data presented here, such as both ventilation perfusion mismatch and true shunt were present with transient blood flow to areas with low V/Q ratios.

We did not perform BAL in this study. We did collect plasma and plan to study the cytokine production as sheep-specific kits become available. We did, however, identify that lipid peroxidation as measured by the Thiobarbituric Acid reactive substances has increased significantly in groups 3 and 4 suggesting that a systemic inflammatory response was underway. There was a 4- to 5-fold increase in neutrophil sequestration as measured by myeloperoxidase activity in pulmonary homogenates in groups 3 and 4. The data from groups 2 and the MIGET study (groups 6 and 7) have not been analyzed yet.

Evidence of lung recruitment on CT has been provided in the slide describing the CT changes in this model.

Copyright © Lippincott Williams & Wilkins. Unauthorized reproduction of this article is prohibited.